Recent climate and air pollution impacts on Indian agriculture

Jennifer Burney[a,1] and V. Ramanathan[b]

[a]School of International Relations and Pacific Studies, University of California, San Diego, La Jolla CA 92093; and [b]Scripps Institution of Oceanography, University of California, San Diego, La Jolla, CA 92037

Edited by Hermann Lotze-Campen, Potsdam Institute for Climate Impact Research, Potsdam, Germany, and accepted by the Editorial Board September 18, 2014 (received for review September 30, 2013)

Recent research on the agricultural impacts of climate change has primarily focused on the roles of temperature and precipitation. These studies show that India has already been negatively affected by recent climate trends. However, anthropogenic climate changes are a result of both global emissions of long-lived greenhouse gases (LLGHGs) and other short-lived climate pollutants (SLCPs). Two potent SLCPs, tropospheric ozone and black carbon, have direct effects on crop yields beyond their indirect effects through climate; emissions of black carbon and ozone precursors have risen dramatically in India over the past three decades. Here, to our knowledge for the first time, we present results of the combined effects of climate change and the direct effects of SLCPs on wheat and rice yields in India from 1980 to 2010. Our statistical model suggests that, averaged over India, yields in 2010 were up to 36% lower for wheat than they otherwise would have been, absent climate and pollutant emissions trends, with some densely populated states experiencing 50% relative yield losses. [Our point estimates for rice (−20%) are similarly large, but not statistically significant.] Upper-bound estimates suggest that an overwhelming fraction (90%) of these losses is due to the direct effects of SLCPs. Gains from addressing regional air pollution could thus counter expected future yield losses resulting from direct climate change effects of LLGHGs.

climate impacts | ozone | aerosols | agriculture | India

Ever since the Green Revolution first staved off famines in the 1960s, Indian rice and wheat systems have grown over the past half century to play critical roles in the world food economy: India's 1.2 billion people depend primarily on food produced within the country, and other Asian and African nations rely heavily on imports of Indian rice. During the 2007–2008 world food price crisis, with wheat harvests failing elsewhere in the world, India banned rice exports out of concern for domestic food security, setting off a worldwide cascade of export bans and food riots. Global food security is thus tightly linked with India's rice and wheat production. In 2008, India produced 148.8 million tons of rice (paddy) and 78.6 million tons of wheat (Fig. S1). In 2006, before the food price spike crisis, India imported over 6 million tons of wheat (~\$1.3 billion) and exported over 4.4 million tons of milled rice (~6.6 million tons of paddy equivalent, ~\$1.5 billion) (1).

Yields for wheat and rice in India have recently begun to level off or even drop in some states (Figs. S2 and S3). This trend, particularly for wheat, counters decades of increasing yields driven by technological innovation (2). At the same time, growing season temperature trends have been positive for major wheat- and rice- producing Indian states (Fig. S4; precipitation trends are mixed). Studies have shown that these climate trends have had a negative impact on Indian agriculture, reducing relative yields by several percent (3, 4). However, although temperature and precipitation changes have and will continue to (5) impact future yields, these two variables alone do not tell the entire story of India's changing crop yields.

Research in the past decade has underscored the critical importance of short-lived climate pollutants (SLCPs)—nonlong-lived greenhouse gases (non-LLGHG) climate warming pollutants—on regional radiative forcing, precipitation, and monsoon patterns (6). SLCPs include black carbon (BC) aerosols as well as the greenhouse gases methane, tropospheric ozone, and hydrofluorocarbons (HFCs); together these compounds have contributed roughly 40% of the current radiative forcing (7, 8). Unlike the LLGHGs, which can persist for centuries in the atmosphere, SLCPs have shorter atmospheric lifetimes—from weeks (black carbon) to months (ozone) or decades (methane and HFCs)—making them appealing mitigation targets (9–11).

SLCPs have indirect effects on agricultural productivity through their impacts on temperature (all) and precipitation (BC). However, BC and ozone are of particular interest for agriculture because they also have direct impacts on crop growth. BC aerosols alter the quantity and nature of the solar radiation reaching the surface (12), and ozone is directly toxic to plants (13). India's breadbasket, the Indo-Gangetic Plains, is subject to a dramatic annual buildup of these (and other) pollutants before the monsoon each year [known as an Atmospheric Brown Cloud, or ABC (6)]. This spatial coincidence is shown in Fig. 1: the most intensively farmed areas in the region area also areas with high average aerosol optical depth and large surface ozone concentrations. Particularly for high-pollution regions like India, understanding the specific role of SLCPs in crop productivity will be critical to assessing the overall impact of climate change and air quality on agriculture and food security.

To our knowledge, this is the first such study to examine both the impacts of climate (temperature and precipitation, or T and P trends) and the direct effects of SLCPs (BC and ozone) on historical yields. Previous work has used statistical models to estimate temperature and precipitation impacts on historical crop yields (3); similar statistical analyses have explored indirect and radiative impacts of ABCs on rain-fed rice yields in India (4, 14).

Significance

Rising temperatures because of increased emissions of long-lived greenhouse gases (LLGHGs) have had and will continue to have significant negative impacts on crop yields. However, other climate changes caused by short-lived climate pollutants (SLCPs) are also significant for agricultural productivity. The SLCPs black carbon and ozone impact temperature, precipitation, radiation, and—in the case of ozone—are directly toxic to plants. To our knowledge, this study provides the first integrated historical examination of the role of both SLCPs and LLGHGs on wheat and rice yields in India, and finds that the majority of losses are attributable to SLCPs. Agricultural cobenefits from SLCP mitigation are expected to be large, and because SLCPs have short atmospheric lifetimes, almost immediate.

Author contributions: J.B. designed research; J.B. performed research; J.B. and V.R. analyzed data; and J.B. and V.R. wrote the paper.

The authors declare no conflict of interest.

This article is a PNAS Direct Submission. H.L.-C. is a guest editor invited by the Editorial Board.

[1]To whom correspondence should be addressed. Email: jburney@ucsd.edu.

This article contains supporting information online at www.pnas.org/lookup/suppl/doi:10.1073/pnas.1317275111/-/DCSupplemental.

SUSTAINABILITY SCIENCE

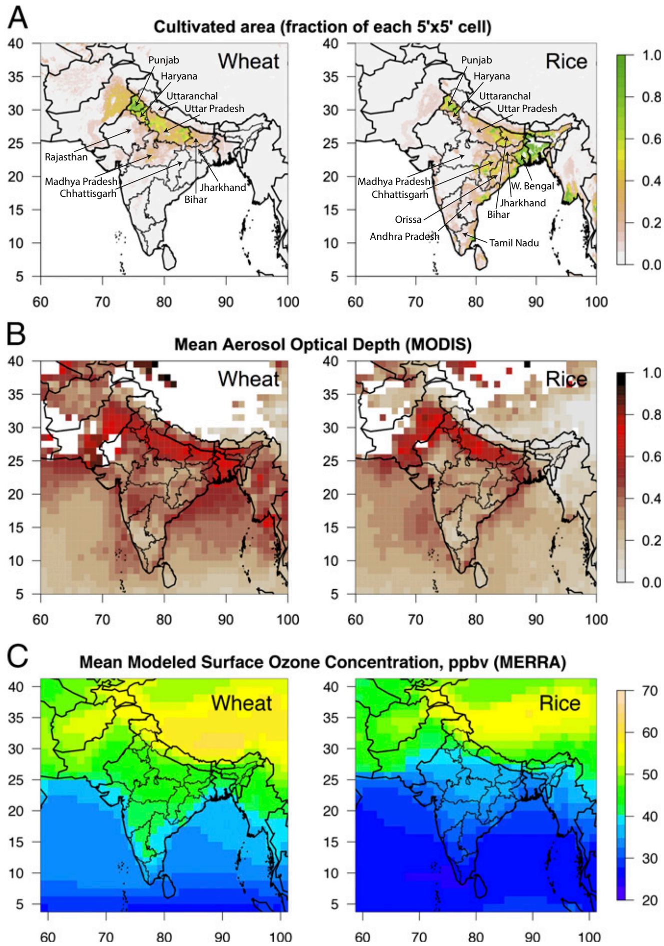

Fig. 1. (*A*) Cultivated fraction of each 5′ x 5′ cell for (*Left*) wheat and (*Right*) rice. States included in this analysis for each crop are labeled. Data are from ref. 58. (*B*) MODIS (Terra) Aerosol Optical Depth at 550 nm in 2008 for (*Left*) March–April–May average, coinciding with the peak of the wheat season, and (*Right*) August–September–October, coinciding with the peak of the kharif rice season. (*C*) Modern-Era Retrospective Analysis (MERRA) estimated 24-h average surface ozone mixing ratio (ppbv) in 2008 for (*Left*) wheat harvest season, March–April–May average, and (*Right*) kharif rice harvest season, August–September–October average (64).

On the ozone side, chamber, open-top, and other field experiments have resulted in hundreds of dose–response relationships for individual crop cultivars over a range of agro-ecological zones and ozone concentrations (15–18). These dose–response relationships have been used to estimate global and regional crop loss in individual years, as well as into the future under different emissions scenarios (11, 19–24). These studies show large ozone impacts: one estimated that global crop loss caused by surface ozone in the year 2000 reached over 79 million metric tons ($11 billion) (21).

In this report, we attempt to harmonize the existing research on climate and pollution impacts on agriculture. We do this by bringing SLCP emissions into a statistical analysis of historical yield data in India for both rice (predominantly rainy season) and wheat (dry season). By explicitly including pollution variables along with climate variables in our analysis, we provide upper-bound estimates of direct SLCP impacts on yields.

Linking SLCP Emissions to Crop Yield Impacts

Although conceptually simple, this quantification of SLCP impacts on crop growth is complicated by: (*i*) the lack of near-surface BC or ozone concentrations over the Indian subcontinent, (*ii*) coemmission and mixing of BC with other aerosol precursors and species, and (*iii*) the nonlinear nature of tropospheric ozone formation. Each of these is discussed briefly below and in greater detail in the *SI Text*.

Emissions Inventories

No long-run records of surface concentrations for BC and ozone exist for India; the best proxy for these pollutant concentrations is therefore an emissions inventory of aerosols and ozone precursor compounds (e.g., refs. 25 and 26). Although not equivalent, emissions of pollutants are nevertheless related to their ambient surface concentrations (e.g., refs. 27–30). Moreover, although crop impacts depend on concentrations, emissions are ultimately the policy-relevant variables; establishment of the link between emissions (as opposed to concentrations) and yields is therefore desirable. The difficulty in this emissions-based approach is then in how to construct emissions variables that can adequately serve as proxies for the basic chemistry and physics governing ozone formation and aerosol radiative impacts.

Black Carbon

The direct impacts of BC on radiation and crop growth are straightforward: BC is an absorbing aerosol that reduces both direct and diffuse light available to plants, and—all else equal—should therefore lower yields. However, this effect is difficult to isolate because BC is usually coemitted or mixes in the atmosphere with other scattering aerosols to create compound particles of varying radiative properties (31). Scattering aerosols also reduce total surface radiation but increase the diffuse fraction; research has shown that plants are often able to more efficiently use diffuse light for photosynthesis (32). Two earlier studies found no significant impact of total surface radiation on rice yields (4, 14). The models in these studies made no distinction between direct and diffuse light, and may have found no effect because the overall reduction in total surface radiation was offset by an enhanced fraction of diffuse radiation. The studies also examined only kharif (rainy season) rice, where expected aerosol impact would be lower.

As with BC, no long-run records exist for the main scattering aerosols: organic carbon (OC) and sulfates. (The main sources of BC in India are domestic biofuels—wood, dung, and crop residues for cooking—and fossil fuels. Biomass burning is also the main source of OC emissions, whereas sulfates are formed from gas-to-particle conversion of sulfur dioxide, SO_2, a main component of coal-fired power plant emissions. Average growing season surface radiation (total = direct + diffuse) for the main wheat- and rice-producing states in India over the past three decades is shown in Figs. S5 and S6 (data are from ref. 33). This dramatic surface dimming of 7–10% is attributed (6, 34) to increased aerosol emissions in the region; total BC+SO_2 emissions and reduction in total surface radiation are correlated with $R^2 = 0.44$. Recent research indicates that the net radiative forcing of OC (once thought to be pure scattering) is in reality close to zero (31), and that the relative abundance of BC and sulfates is the main determinant of overall aerosol radiative forcing (35). We therefore include BC and SO_2 emissions (as the main precursor for sulfate aerosols) in our model, and omit OC.

Ozone

Tropospheric ozone (O_3) formation depends on the presence of methane, carbon monoxide, or volatile organic compounds (VOCs) and nitrogen oxides (NOx = NO + NO_2). [We use NOx and nonmethane VOCs (NMVOCs) in our analysis because CO and methane (CH_4) contribute predominantly to background ozone levels.] At low NOx concentrations, increasing levels of NOx and, to a lesser extent NMVOCs, result in higher ozone concentrations. At high NOx concentrations, increased NOx can conversely result in net titration of ozone out of the atmosphere, bringing overall levels down (with changes in NMVOC concentrations having little impact). The determinant of these two NOx "regimes" is the ratio of summed VOCs (weighted by reactivity) to NOx (36). Our model therefore includes NOx, NMVOCs, and the NMVOC:NOx ratio.

No long-run records of either surface ozone or ozone precursor concentrations exist for India, but global background levels of tropospheric ozone are increasing in general (37), and several site-specific measurements in India corroborate this trend (38, 39). Emissions of all ozone precursors are rising in India, with NOx emissions outpacing NMVOCs; the ratio of these two precursors varies dramatically across the country (Fig. S7). The main sources of NOx emissions are the transportation sector and coal combustion; VOCs are emitted in biomass combustion, a large variety of industrial processes, and in vehicle exhaust. (It should also be noted that NOx is a strong oxidant and damaging to plants on its own.) Figs. S5–S8 show trends and spatial distribution of BC, SO_2, NOx, and NMVOC emissions.

Model Overview

To quantify the impacts of climate and air pollution trends on Indian agricultural production, we constructed a dataset of rice and wheat yields, surface air temperature, precipitation, and aerosol and ozone precursor emissions for major Indian wheat- and rice-producing states from 1980 to 2010. Fig. 1*A* shows the states included in the analysis. To relate climate and air pollution to crop yields, we followed techniques well established in the literature (3, 4, 14, 40) and regressed state-level wheat and rice yields in India on weather and emissions variables using the basic regression model:

$$ln(Y_{it}) = \vec{\beta} \times \vec{X}_{it} + S_i + f_i(t) + \epsilon_{it}.$$

In this specification, Y_{it} is crop yield (kilograms/hectare of either wheat or rice) for state i in year t, ϵ_{it} are the error terms, and the β-coefficients are the terms of interest minus the state-independent coefficients for dependence of yield on the climate and pollution variables, X_{it}. Log-transforming Y_{it} normalizes the distributions and makes results interpretable across orders of magnitude (i.e., as percent changes). S_i are state-fixed effects (state-specific intercepts), which control for time-invariant differences between states like soil type; $f_i(t)$ are time controls, which account for time-varying differences between states like rates of technology adoption, governance, policy, and so forth (we use state-specific linear and quadratic time trends, with other specifications presented in *SI Text*). [Previous studies using statistical panel models to estimate climate impacts on agriculture have similarly included region-specific and pooled quadratic time trends to capture a general empirical leveling-off of yields (3, 4, 14, 40). Because these previous studies have not included SLCPs explicitly, they implicitly capture SLCP direct impacts with the quadratic time terms meant to capture unaccounted-for technology effects. Moreover, all such panel studies—this one included—implicitly capture SLCP indirect impacts in the coefficients for temperature and precipitation.]

The climate and emissions variables included in our model are: T and P (average growing season temperature and precipitation), T^2 and P^2 (average growing season temperature-squared and precipitation-squared as measures of extremes), $ln(SO_2)$ and $ln(BC)$ (emissions as aerosol concentration proxies), and $ln(NOx)$, $ln(NMVOC)$, and the ratio of those two terms. Satellite and European air quality monitoring station data are used to justify the ozone specification in the model, to determine appropriate functional form, and to verify the existence of both NOx regimes over the study area, as described in Fig. 2 and below.

To contextualize our regression analysis, we then calculated the relative yield change (RYC) in 2010 as the percentage change between our model predictions and a counterfactual scenario without long-run climate and pollution trends (i.e., we use our model to project yields from 1980 to 2010, with climate and emissions variables held at average 1980 levels). We compared the 2006–2010 average for both real-world and counterfactual scenarios to more accurately reflect long-run differences. We then weighted the state-level RYC results by either crop area or production (both weightings are presented below) and summed to derive national-level yield impacts of recent climate and pollution trends.

Results

Relative Impacts of Climate and Pollution at the National Level. The main results of our analysis are presented in Fig. 3, with full regression results in Table S1. Average (median) RYC is plotted as red diamonds, with error bars calculated by bootstrapping the model 1,000 times (clustered on years, with replacement) and selecting the 5th–95th percentile range. Ex ante, we would expect to see larger impacts on wheat than rice for two reasons: (*i*) wheat's main growing season coincides with the greatest buildup of pollution over the Indian subcontinent; and (*ii*) wheat shows more sensitivity than rice to ozone in chamber experiments. Indeed, we found that wheat yields were over 36% lower in 2010 than they would have been absent climate and SLCP emissions trends (−36.92% weighted by area; −37.91 weighted by production). For rice, our median estimates suggest that yields were over 20% lower (−20.56 weighted by area; −20.85 weighted by production), but the 5th–95th confidence interval includes zero for rice. Our analysis indicates that 90% of the RYC in wheat can be attributed to SLCPs (Fig. 3, yellow bars), as opposed to trends in average temperature and precipitation (Fig. 3, blue bars).

At the country level our findings for climate (T and P) impacts over this time period (RYC of −3.5% for wheat and minimal for rice) are similar to previous studies (3, 4, 14). We find that a 1 °C increase in temperature leads to a yield decline on average of 4% for wheat and 5% for rice. The coefficients for temperature (Table S1) are statistically significant for both crops; precipitation is not statistically significant for either. [Significance at 90% with standard errors corrected for spatial and serial correlation (41).] The climate portion of the RYC for wheat may be a lower-bound, given that irrigation mitigates some temperature impact through soil moisture (42).

It is less straightforward to compare our results for aerosol and ozone precursor effects to previous studies. Two earlier studies found no significant impact of total surface radiation on rice yields (4, 14). The models in these studies made no distinction between direct and diffuse light, and may have found no effect because the overall reduction in total surface radiation was offset by an enhanced fraction of diffuse radiation, which plants use more efficiently for photosynthesis. The studies also examined only kharif (rainy season) rice, where expected aerosol impact would be lower. The coefficients for our preferred model specification (Eq. **1**), in which sulfates and BC are accounted for separately, are negative for wheat, and statistically significant. Auffhammer et al. (14) found that ABCs resulted in a RYC of −6% over 30 y (14) for rain-fed rice in India. Although the total impact of aerosols varies a bit depending on model specification, we find a similar magnitude impact.

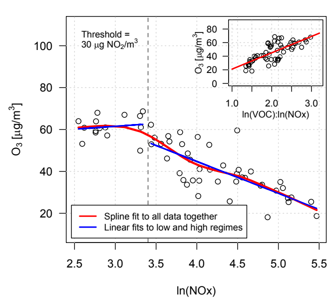

Fig. 2. Relationship between yearly mean ozone and precursor concentrations at European monitoring stations observing ozone, NOx, and NMVOCs. Main plot shows the existence of low- and high-NOx regimes (with opposite-signed relationships). (*Inset*) The relationship between ozone and the NMVOC:NOx ratio. These data were used to guide choice of functional form in our model. Data from AirBase v.6 (65).

SUSTAINABILITY SCIENCE

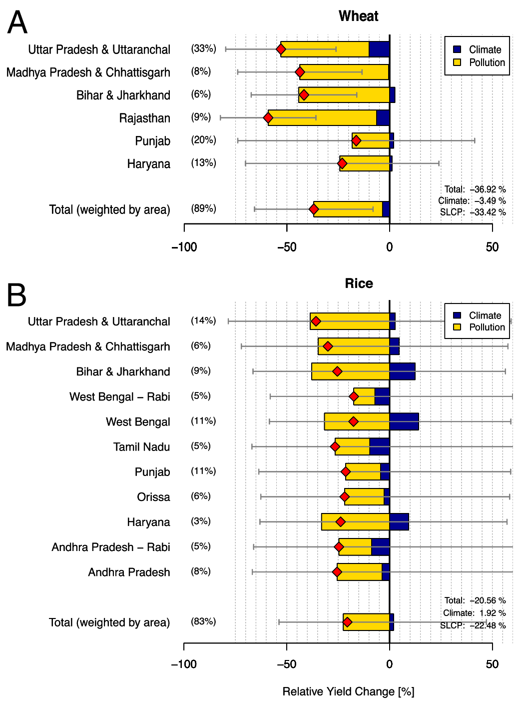

Fig. 3. RYC resulting from climate and SLCPs for (*A*) wheat and (*B*) rice. For both crops, RYC is calculated as [$\text{Model}_{(2006\text{–}2010\ \text{avg})} - \text{Baseline}_{(2006\text{–}2010\ \text{avg})}$]/$\text{Baseline}_{(2006\text{–}2010\ \text{avg})}$ (plotted as red diamonds). The portion of the total yield change because of temperature and precipitation trends (blue bars) is estimated using the coefficients in Table S1 and the average trends in *T* and *P* (Fig. S4). The remainder is a result of SLCPs. Country totals are estimated by summing state values weighted by total area. Error bars are constructed for each state by bootstrap resampling the model 1,000 times and selecting the 95% range.

Ozone precursor emissions are significant for both crops. No previous studies have examined the statistical historical relationship between ozone precursor emissions and crop yields, but several studies have used chemical transport models to simulate atmospheric ozone concentrations, and have then applied concentration–response relationships derived from field experiments to estimate crop loss caused by ozone exposure (19–22). Van Dingenen et al. estimate 7–12% for wheat and 3–4% for rice in the year 2000 (20); Avnery et al. estimate that in the year 2000, surface ozone reduced global wheat production by 3.9–15% (21), with additional RYC between 2030 and 2000 up to −26% (22), very similar to our estimates (which also include aerosol impacts).

State-by-State Variation. There is substantial variation in relative impacts of climate and SLCPs across states. Some of the most dramatic impacts for both wheat and rice have occurred in Uttar Pradesh and Uttaranchal (UP). UP, India's most populous state, is the largest producer of both wheat and rice in the country, providing over one-third of India's wheat and 14% of India's rice. In particular, wheat yields for UP are ∼50% lower than they otherwise would have been absent climate and pollution trends, and over two-thirds of that RYC is attributable to SLCP emissions trends (state-by-state time projections are shown in Fig. S9).

Rajasthan, although producing a lower percentage of India's wheat, shows the greatest overall wheat RYC (more than 50%). The relatively large climate impacts on wheat in both UP and Rajasthan are driven by temperature, as the two states have had the largest increases in growing season temperature since 1980 (Fig. S4) (0.87° for Rajasthan and 0.52° for UP). Four of the main wheat-producing states—UP, Rajasthan, Madhya Pradesh and Chhattisgarh, and Bihar and Jharkhand—have large negative SLCP impacts, whereas Punjab and Haryana show little to no impact of either SLCPs or climate (not statistically significant at 90%). Moreover, the uncertainties in Punjab and Haryana are greater than for other states, and across alternative models specifications (Figs. S10–S12). Two factors likely explain these differences. First, Punjab and Haryana are the most technologically advanced wheat-producing states in India, with the highest yields and the greatest yield gains over the time period (Fig. S2); they also feature some of the lowest estimated crop yield gaps in India (and the world) (43), meaning they have been closest to achieving biological potential despite climate and emissions changes (Fig. S9). However, in addition, the intricacies of ozone production likely explain the SLCP impact differences (see below).

For rice, the overall climate and pollution impacts are lower, and the state-by-state variation is less than for wheat (see also Fig. S13 for kharif-only analysis). Most notably, the southeastern states of Tamil Nadu and Andhra Pradesh show higher relative climate impacts; these are two of the least-polluted states in the study region (e.g., Fig. 1 and Figs. S5–S8); they have also featured significant growing season temperature increases (Fig. S4). The states of the heavily polluted northern and eastern Indo Gangetic Plains (UP, Bihar and Jharkhand, West Bengal) all exhibit SLCP RYC of −15% or more. Haryana and Punjab, the two states with the smallest SLCP impacts in wheat, do not diverge from the other states in rice impacts. The difference in SLCP impacts between the two crops for Punjab and Haryana is likely dominated by differences in rates of ozone formation in the two states between the two seasons.

Studies suggest that in the summer monsoon months NOx and ozone concentrations are higher than in winter, and remain higher in those two states than elsewhere (44–46). This finding may be because of higher temperatures (47) and higher concentrations of NMVOCs from biomass burning (48, 49) [traditionally one of the biggest sources of uncertainty in emissions inventories (50)] during the rice growing season. Additionally, the possibility exists that farmers in these two states may be adapting wheat crops more successfully than rice crops by selecting cultivars with higher ozone resistance (although such potential is limited) (23, 51).

As shown in Fig. S7, NOx and NMVOC emissions have risen fairly steadily in all six states, but the ratio of the two differs across states. In particular, we expect states with higher NMVOC:NOx ratios to have higher ozone concentrations and therefore higher RYC, but states with very high NOx concentrations are at the very least VOC-sensitive regimes, and might actually have net titration of ozone from the atmosphere (See *SI Text* for a more detailed discussion). Punjab and Haryana have very high NOx emissions, but low NMVOC:NOx ratios, whereas the other four states have lower overall NOx emissions but higher NMVOC:NOx ratios.

We examined satellite data to confirm the plausibility of differential ozone impacts across states. Previous work (30) showed that the ratio of columnar formaldehyde (HCHO) to nitrogen dioxide (NO_2) was a suitable proxy for the VOC:NOx ratio and could be used to distinguish NOx-sensitive from NOx-saturated regimes. We replicated this methodology using data from the Ozone Monitoring Instrument (52) and found that the relationship between columnar ozone and NO_2 switches sign at the HCHO:NO_2 value of ∼4. As shown in Fig. 4, satellite data from 2008 indicate that the northwestern Indo-Gangetic Plain (Punjab/Haryana) has a lower HCHO:NO_2 ratio than the eastern Indo-Gangetic Plain (e.g., UP/Bihar). Indeed, for most of the wheat-growing season, much of Punjab and Haryana is NOx-saturated (whereas both are NOx-sensitive during the rice growing season). These satellite data confirm the existence of different NOx regimes across India during the wheat season, and thus provide additional support for our preferred model specification (as opposed to a simpler specification that simply included precursors together or omitted the VOC:NOx ratio). Further research is needed to fully flesh out these dynamics, particularly as panel statistical analyses are becoming the tool of choice for agricultural impact assessments.

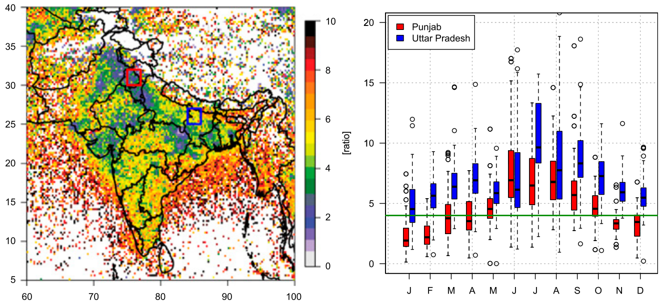

Fig. 4. (*Left*) Map of India showing average December–January–February HCHO:NO_2 ratio. The 2° cells in Punjab (red) and UP/Bihar (blue) are used for comparative analysis in the right panel. (*Right*) Distribution of HCHO:NO_2 ratio in grid cells in two comparison regions for 2008, by month. The line (ratio = 4) represents the empirically derived transition between ozone titrating (i.e., the relationship between columnar ozone and NO_2 is negative) and NOx-sensitive (the relationship is positive) regimes. In the wheat-growing season, Punjab/Haryana is largely NOx-saturated, whereas UP/Bihar is NOx-sensitive.

Discussion

Several caveats to this analysis exist. First, meso-scale transport of pollutants by winds to neighboring states could skew results (11, 53). This is an important subject for future research, as the policy implications for local and transported pollutant impacts would be quite different. A more comprehensive surface ozone and SLCP monitoring network could be used to investigate the origins of pollution by examining the correlation between local emissions, local tropospheric O_3 formation, and direct/diffuse radiation; these data could in turn be used to cross-check chemical transport models and to create observationally constrained emissions inventories. Second, this analysis ignores interdependencies between several of the independent variables: for example, ozone formation is a function of temperature as well as precursor concentrations; precipitation removes aerosols from the atmosphere.

Most important, as with any statistical analysis, our results depend on model specification and choice of a baseline (or counterfactual) scenario. Our model includes state-specific linear and quadratic time trends, allowing for unknown variables—like technology and policy changes—to account for the slope and curvature of yield trends in each state. For our baseline scenario, we use the coefficients from our model to project yields forward, absent the long-run trends in emissions, temperature, and precipitation. We thus assume that these time trends in the counterfactual scenario are independent of pollution and emissions trends; this is likely untrue because industrialization and mechanization likely contributed both to increased emissions and to higher yields. For this reason, we consider our estimates to be upper-bounds.

Finally, our analysis is statistically limited in two key ways. First, the study area is geographically small (i.e., the number of observational units is low), and second, emissions trends have been similar across the region, limiting the amount of information that can be gleaned from this scale of analysis. These limitations are discussed in greater detail in *SI Text*, Tables S2 and S3, and Fig. S14.

Our results nevertheless indicate that SLCPs have had significant impact on crop yields in India in recent decades. The main wheat-producing state (UP) has been hit especially hard; rice-producing states in the heavily polluted northern Indo-Gangetic Plains have also been significantly negatively affected. For context, the yield loss for wheat attributable to SLCPs alone in 2010 (−18.9%) corresponds to over 24 million tons of wheat: around four times India's wheat imports before the 2007–2008 food price crisis and a value of ~\$5 billion. Mitigation of SLCP emissions in India could thus have important food security impacts both domestically and internationally. Impacts on Chinese agriculture would be similarly large, as emissions of SLCPs by China are larger by a factor of two to three (for a smaller total arable land area). Finally, under the simplistic assumption that India's 2010 wheat yield loss was compensated for by cropland expansion and increased production elsewhere, an additional 1.1 GtC (as CO_2) would have been released into the atmosphere from land conversion alone (using global averages) (54).

To our knowledge, this analysis for the first time decouples the historical impacts of climate and pollution, and thus offers a grounded, upper-bound assessment of SLCP mitigation potential. Yield increases from reduction of air pollution could help offset anticipated future expected yield losses resulting from temperature and precipitation changes. In the short term, this is an appealing option because SLCP mitigation will produce immediate results that can help counter the impacts of climate changes and sea level rise (55) already "locked in" from historical LLGHG and SLCP emissions. In the long term, although farmers may select/breed more pollution-resilient cultivars or alter management practices to help minimize such losses (51, 56), air pollution mitigation—particularly of ozone precursors—will become an ever-more important food security measure.

Materials and Methods

We constructed state-level climate and pollutant variables by averaging gridded temperature, precipitation, and emissions data over crop area and growing season for each crop and aggregating to the state level (Figs. S4–S7; to give an idea of spatial heterogeneity, average emissions of SO_2, BC, NOx, and NMVOCs during the wheat season for 2008 are shown in Fig. S8). Wheat is a winter crop in India; it is planted in November–December and then harvested in March, April, and May. This is the dry season, and almost all wheat in India is irrigated. Indian rice is grown in two main seasons. The main kharif rice crop (in which over 85% of rice is produced) coincides with the monsoonal rains: planting occurs in May–June and harvest is August, September, and October. The second rabi rice crop is a winter crop, roughly coinciding with the wheat season. We gathered state-level yield data for wheat, kharif rice, and rabi rice, and grouped them for analysis by crop (i.e., one analysis for wheat, and one for rice, including kharif and rabi). For rice, we used the entire period between planting and harvesting as the growing season; for wheat, we used the 120 d before harvest, in agreement with previous work (3). We use 1979 boundaries for Indian states in this analysis, with states that split after 1979 (e.g., Bihar and Jharkhand, UP, and Madhya Pradesh and Chhattisgarh) considered together for the period of analysis. The states included in this analysis (Fig. 1) represent over 80% of rice production/area and over 85% wheat production/area.

State-level yield, production, and area data for India are from IndiaStat.com, aggregated from state and national agricultural ministries (57). Gridded crop area estimates (58) give the percentage of each 5-min cell devoted to each crop, and crop growing season data (59) gives planting and harvesting dates at 5-min resolution for all major crops. Temperature and precipitation data are taken from the Monthly Air Temperature and Monthly Total Precipitation Time Series (1900–2010) compiled by the University of Delaware climate research group (0.5 × 0.5 monthly averages) (60). Gridded emissions of SO_2, BC, NOx, and NMVOCs are annual historical estimates from the Regional Emissions Inventory in Asia at 0.5 × 0.5 resolution, available monthly from 1980 to 2010 (26). [We repeat our analysis using an alternative climate dataset (61), maximum and minimum temperatures (61, 62), and an alternative emissions inventory (63), as robustness checks in the *SI Text*.] Solar radiation data (Figs. S5 and S6) was provided by the World Radiation Data Center (33). Sites with data covering the entire period were used, including (India) Ahmadabad, Bhaunagar, Bombay, Calcutta, Goa, Jodhpur, Kodiakanal, Madras, Nagpur, New Delhi, Poona, Shillong, Trivandrum, Vishakhapatnam, (Pakistan) Lahore City, and (Sri Lanka) Colombo. Daily global radiation data were averaged and monthly values interpolated across the region with the edges of the region set to the median values.

ACKNOWLEDGMENTS. We thank numerous anonymous reviewers for helpful feedback on the manuscript. This work was supported by the University of California President's Postdoctoral Fellowship Program and the National Science Foundation (Grant AGS1016496).

1. Food and Agriculture Organization of the United Nations, Food and Agriculture Organization of the United Nations Statistical Database (FAOSTAT). Available at www.faostat.org. Accessed June 5, 2014.
2. Lin M, Huybers P (2012) Reckoning wheat yield trends. *Environ Res Lett* 7(2):024016.
3. Lobell DB, Schlenker W, Costa-Roberts J (2011) Climate trends and global crop production since 1980. *Science* 333(6042):616–620.
4. Auffhammer M, Ramanathan V, Vincent J (2012) Climate change, the monsoon, and rice yield in India. *Clim Change* 111(2):411–424.
5. Lobell DB, et al. (2008) Prioritizing climate change adaptation needs for food security in 2030. *Science* 319(5863):607–610.
6. Ramanathan V, et al. (2005) Atmospheric brown clouds: Impacts on South Asian climate and hydrological cycle. *Proc Natl Acad Sci USA* 102(15):5326–5333.
7. Forster P, et al. (2007) Climate change 2007: The physical science basis. *Contribution of Working Group I to the Fourth Assessment Report of the Intergovernmental Panel on Climate Change*, eds Solomon S, et al. (Cambridge Univ Press, Cambridge, UK).
8. Ramanathan V, Xu Y (2010) The Copenhagen Accord for limiting global warming: Criteria, constraints, and available avenues. *Proc Natl Acad Sci USA* 107(18):8055–8062.
9. Wallack JS, Ramanathan V (2009) The other climate changers: Why black carbon and ozone also matter. *Foreign Affairs* 88(5):105–113.
10. United Nations Environment Programme and World Meteorological Organization (2011) *Integrated Assessment of Black Carbon and Tropospheric Ozone* (United Nations Office at Nairobi Publishing Services Section, Nairobi).
11. Shindell D, et al. (2012) Simultaneously mitigating near-term climate change and improving human health and food security. *Science* 335(6065):183–189.
12. Ramanathan V, Carmichael G (2008) Global and regional climate changes due to black carbon. *Nat Geosci* 1(4):221–227.
13. Ainsworth EA, Yendrek CR, Sitch S, Collins WJ, Emberson LD (2012) The effects of tropospheric ozone on net primary productivity and implications for climate change. *Annu Rev Plant Biol* 63:637–661.
14. Auffhammer M, Ramanathan V, Vincent JR (2006) Integrated model shows that atmospheric brown clouds and greenhouse gases have reduced rice harvests in India. *Proc Natl Acad Sci USA* 103(52):19668–19672.
15. Mills G, et al. (2007) A synthesis of AOT40-based response functions and critical levels of ozone for agricultural and horticultural crops. *Atmos Environ* 41(12):2630–2643.
16. Emberson L, et al. (2009) A comparison of North American and Asian exposure-response data for ozone effects on crop yields. *Atmos Environ* 43(12):1945–1953.
17. Pleijel H, Danielsson H, Emberson L, Ashmore M, Mills G (2007) Ozone risk assessment for agricultural crops in Europe: Further development of stomatal flux and flux–response relationships for European wheat and potato. *Atmos Environ* 41(14):3022–3040.
18. Grünhage L, et al. (2012) Updated stomatal flux and flux-effect models for wheat for quantifying effects of ozone on grain yield, grain mass and protein yield. *Environ Pollut* 165:147–157.
19. Wang X, Mauzerall DL (2004) Characterizing distributions of surface ozone and its impact on grain production in China, Japan and South Korea: 1990 and 2020. *Atmos Environ* 38(26):4383–4402.
20. Van Dingenen R, et al. (2009) The global impact of ozone on agricultural crop yields under current and future air quality legislation. *Atmos Environ* 43(3):604–618.
21. Avnery S, Mauzerall DL, Liu J, Horowitz LW (2011) Global crop yield reductions due to surface ozone exposure: 1. Year 2000 crop production losses and economic damage. *Atmos Environ* 45(13):2284–2296.
22. Avnery S, Mauzerall DL, Liu J, Horowitz LW (2011) Global crop yield reductions due to surface ozone exposure: 2. Year 2030 potential crop production losses and economic damage under two scenarios of o3 pollution. *Atmos Environ* 45(13):2297–2309.
23. Avnery S, Mauzerall DL, Fiore AM (2013) Increasing global agricultural production by reducing ozone damages via methane emission controls and ozone-resistant cultivar selection. *Glob Change Biol* 19(4):1285–1299.
24. Ghude S, et al. (2014) Reduction in India's crop yield due to ozone. *Geophys Res Lett* 41(15):5685–5691.
25. EC-JRC/PBL (2011) Emission Database for Global Atmospheric Research (EDGAR), release version 4.2. Available at edgar.jrc.ec.europa.eu/overview.php?v=42. Accessed April 30, 2012.
26. Ohara T, et al. (2007) An Asian emission inventory of anthropogenic emission sources for the period 1980–2020. *Atmos Chem Phys* 7:4419–4444.
27. Hilboll A, Richter A, Burrows JP (2013) Long-term changes of tropospheric NO_2 over megacities derived from multiple satellite instruments. *Atmos Chem Phys* 13:4145–4169.
28. Menon S, et al. (2010) Black carbon aerosols and the third polar ice cap. *Atmos Chem Phys* 10:4559–4571.
29. Duncan BN, Martin RV, Staudt AC, Yevich R, Logan JA (2003) Interannual and seasonal variability of biomass burning emissions constrained by satellite observations. *J Geophys Res* 108(D2):ACH1-1–ACH1-22.
30. Martin RV, Fiore AM, Van Donkelaar A (2004) Space-based diagnosis of surface ozone sensitivity to anthropogenic emissions. *Geophys Res Lett* 31(6):L06120.
31. Chung CE, Ramanathan V, Decremer D (2012) Observationally constrained estimates of carbonaceous aerosol radiative forcing. *Proc Nat Acad Sci USA* 109(29):11624–11629.
32. Mercado LM, et al. (2009) Impact of changes in diffuse radiation on the global land carbon sink. *Nature* 458(7241):1014–1017.
33. World Radiation Data Center (WRDC), Global Radiation Data. Available at wrdc.mgo.rssi.ru. Accessed June 9, 2011.
34. Padma Kumari B, Londhe AL, Daniel S, Jadhav DB (2007) Observational evidence of solar dimming: Offsetting surface warming over India. *Geophys Res Lett* 34(21):L21810.
35. Ramana MV, et al. (2010) Warming influenced by the ratio of black carbon to sulphate and the black-carbon source. *Nat Geosci* 3(8):542–545.
36. Sillman S (1999) The relation between ozone, NOx and hydrocarbons in urban and polluted rural environments. *Atmos Environ* 33(12):1821–1845.
37. Vingarzan R (2004) A review of surface ozone background levels and trends. *Atmos Environ* 38(21):3431–3442.
38. Lal S, Naja M, Subbaraya B (2000) Seasonal variations in surface ozone and its precursors over an urban site in India. *Atmos Environ* 34(17):2713–2724.
39. Chakrabarty DK, Peshin SK, Pandya KV, Shah NC (1998) Long-term trend of ozone column over the Indian region. *J Geophys Res* 103(D15):19245–19251.
40. Schlenker W, Lobell DB (2010) Robust negative impacts of climate change on African agriculture. *Environ Res Lett* 5(1):014010.
41. Hsiang SM (2010) Temperatures and cyclones strongly associated with economic production in the Caribbean and Central America. *Proc Natl Acad Sci USA* 107(35):15367–15372.
42. Lobell DB, et al. (2013) The critical role of extreme heat for maize production in the United States. *Nat Clim Change* 3(5):497–501.
43. Lobell DB, Cassman KG, Field CB (2009) Crop yield gaps: Their importance, magnitudes, and causes. *Annu Rev Environ Resour* 34:179–204.
44. Ghude SD, Fadnavis S, Beig G, Polade SD, van der A RJ (2008) Detection of surface emission hot spots, trends, and seasonal cycle from satellite-retrieved NO_2 over India. *J Geophys Res* 113(D20):D20305.
45. Beig G, Ali K (2006) Behavior of boundary layer ozone and its precursors over a great alluvial plain of the world: Indo-Gangetic Plains. *Geophys Res Lett* 33(24):L24813.
46. Kulkarni PS, et al. (2009) On some aspects of tropospheric ozone variability over the Indo-Gangetic (IG) basin, India. *Int J Remote Sens* 30(15-16):4111–4122.
47. Sillman S, Samson PJ (1995) Impact of temperature on oxidant photochemistry in urban, polluted rural and remote environments. *J Geophys Res* 100(D6):11497–11508.
48. Streets DG, Yarber KF, Woo JH, Carmichael GR (2003) Biomass burning in Asia: Annual and seasonal estimates and atmospheric emissions. *Global Biogeochem Cy* 17(4):1099.
49. Venkataraman C, et al. (2006) Emissions from open biomass burning in India: Integrating the inventory approach with high-resolution moderate resolution imaging spectroradiometer (MODIS) active-fire and land cover data. *Global Biogeochem Cy* 20(2):GB2013.
50. Bond TC, et al. (2013) Bounding the role of black carbon in the climate system: A scientific assessment. *J Geophys Res Atmos* 118(11):5380–5552.
51. Teixeira E, et al. (2011) Limited potential of crop management for mitigating surface ozone impacts on global food supply. *Atmos Environ* 45(15):2569–2576.
52. NASA, Ozone Monitoring Instrument (OMI). Available at disc.sci.gsfc.nasa.gov/giovanni. Accessed July 15, 2013.
53. Hollaway MJ, Arnold SR, Challinor AJ, Emberson LD (2012) Intercontinental transboundary contributions to ozone-induced crop yield losses in the northern hemisphere. *Biogeosciences* 9:271–292.
54. Burney JA, Davis SJ, Lobell DB (2010) Greenhouse gas mitigation by agricultural intensification. *Proc Natl Acad Sci USA* 107(26):12052–12057.
55. Hu A, Xu Y, Tebaldi C, Washington WM, Ramanathan V (2013) Mitigation of short-lived climate pollutants slows sea-level rise. *Nat Clim Change* 3(8):730–734.
56. Lobell DB, Ortiz-Monasterio JI, Sibley AM, Sohu V (2013) Satellite detection of earlier wheat sowing in India and implications for yield trends. *Ag Sys* 115:137–143.
57. Datanet India, IndiaStat. Available at www.indiastat.com. Accessed July 17, 2012.
58. Monfreda C, Ramankutty N, Foley JA (2008) Farming the planet: 2. Geographic distribution of crop areas, yields, physiological types, and net primary production in the year 2000. *Global Biogeochem Cy* 22(1):GB1022.
59. Sacks WJ, Deryng D, Foley JA, Ramankutty N (2010) Crop planting dates: An analysis of global patterns. *Glob Ecol Biogeogr* 19(5):607–620.
60. University of Delaware, Global Climate Data. Available at climate.geog.udel.edu/∼climate. Accessed June 8, 2012.
61. Climatic Research Unit, High-Resolution Gridded Climate Datasets (CRU TS3.21). Available at www.cru.uea.ac.uk/cru/data/hrg. Accessed May 5, 2014.
62. Welch JR, et al. (2010) Rice yields in tropical/subtropical Asia exhibit large but opposing sensitivities to minimum and maximum temperatures. *Proc Natl Acad Sci USA* 107(33):14562–14567.
63. Lu Z, Zhang Q, Streets DG (2011) Sulfur dioxide and primary carbonaceous aerosol emissions in China and India, 1996–2010. *Atmos Chem Phys* 11:9839–9864.
64. NASA, MERRA: Modern-Era Retrospective-Analysis for Research and Applications. Available at disc.sci.gsfc.nasa.gov/giovanni. Accessed July 20, 2012.
65. European Environment Agency Topic Centre on Air Pollution and Climate Change Mitigation, AirBase, version 6.0. Available at acm.eionet.europa.eu/databases/airbase. Accessed February 25, 2013.

Supporting Information

Burney and Ramanathan 10.1073/pnas.1317275111

SI Text

Model Details. Our model includes state fixed effects (S_i in Eq. **1**) to account for time-invariant differences across the region (e.g., soil type), and state-specific linear and quadratic time trends [$f(t)$] to account for divergent evolution of policies, infrastructure, and management over time between states. We do not explicitly include any technology or management variables (e.g., fertilizer application rates, use of high-yielding varieties, irrigation coverage, and so forth) in any of the models because these changes are captured to some extent in the state-specific time trends. The inclusion of the linear time term effectively detrends the data so that we are not simply correlating increasing quantities (yield, temperature, emissions, and so forth). The inclusion of the quadratic term allows for the possibility that other nonclimate, nonpollution factors may contribute to a leveling-off of yields. Because the dependent variable (Y_{it}) is logged, we can interpret results in terms of percent changes in yield.

Our model includes both climate and pollution variables: T and P, the average growing season temperature and precipitation, as well as T^2 and P^2, the average growing season temperature-squared and precipitation-squared. Inclusion of these squared terms to some degree accounts for extreme temperature and precipitation events and also ensures that our model accounts for weather variations across sites, and not just within sites (1). We standardize T and P by subtracting their means and dividing by their standard deviations (SDs). This approach allows us to interpret the regression coefficients in terms of SDs [i.e., a +1 SD change in T results in a $(\beta_T + 2 * \beta_{T^2}) * 100\%$ change in Y]. The other variables used are: $ln(SO_2)$, average sulfur dioxide emissions (kg m^{-2} s^{-1}); $ln(BC)$, the average BC emissions (kg m^{-2} s^{-1}); $ln(NMVOC)$, the average emissions of nonmethane volatile organic compounds (kg m^{-2} s^{-1}); $ln(NOx)$, the average emissions of nitrogen oxides (kg m^{-2} s^{-1}); and the ratio $ln(NMVOC)$: $ln(NOx)$. The use of logged emissions variables allows for the interpretation of regression coefficients in terms of elasticities; that is, a 1% change in sulfur dioxide emissions leads to a $\beta_{SO_2}\%$ change in yield, and so forth. The physical meaning of the pollution variables (including physical rationale for the logged form) is discussed in greater detail below; sources for all of the above-mentioned data can be found in *Materials and Methods*. As described in *Materials and Methods*, emissions are aggregated over crop area and growing season (for either wheat or rice) to the state-year from monthly gridded datasets.

To calculate the impacts of climate and pollution on yields, we calculated the percent change between predicted values from our main model and predicted values from a baseline scenario. (RYC is calculated using average 2006–2010 values for both model and baseline to avoid influence of fluctuations.) The baseline scenario is counterfactual: it includes only historical technology trends and effectively holds T, P, and aerosol and ozone precursor emissions at 1980 levels (average 1980–1981 levels, to avoid having results influenced by endpoints). These results are presented in Fig. 3. Error bars (90% confidence) are constructed by bootstrap resampling the model 1,000 times and selecting the 5th–95th percentile range. To calculate overall impacts, we summed the state-wide percent changes weighted by area (e.g., totals in Fig. 3) or production (numbers given in main text).

Emissions Variables, Aerosols, and Tropospheric Ozone Chemistry. ***Aerosols.*** Our models give a more complete accounting than previous work (2, 3) of the impacts of short-lived climate forcers on surface radiation by including gridded emissions of sulfur dioxide (SO_2) and black carbon (BC) as markers for surface radiation changes. We include SO_2 as a proxy for sulfate aerosols, because it is the main anthropogenic precursor to sulfates (atmospheric sulfate ions are formed by photochemical oxidation of SO_2 followed by gas-to-particle conversion). BC is a by-product of biomass and fossil fuel combustion (especially diesel); it can be found in the atmosphere in pure (BC) form or in various mixtures with organic carbon (OC) compounds and sulfates. We do not include OC here as it usually appears as Brown Carbon (BrC), the radiative properties of which vary (4).
Ozone precursors. Tropospheric ozone (O_3) forms when ozone precursor compounds react in the presence of sunlight. Formation is highly localized and depends on the presence of both volatile organic compounds (VOCs) or carbon monoxide (CO) and nitrogen oxides ($NOx = NO + NO_2$). (We use VOCs for the remainder of this discussion, although as noted CO can substitute for a VOC in the initial reaction. See below for alternate ozone specifications.) Formation is triggered when a VOC reacts with OH in the atmosphere to form a peroxy radical. These radicals (the hydroxyl, HO_2, is the simplest of the family, represented in general by RO_2) then combine with NO to produce NO_2. At lower NOx concentrations, in the presence of sunlight, NO_2 is photolyzed, providing the extra O that combines with O_2 to form ozone. At high NOx concentrations, NO conversely titrates ozone out of the atmosphere, pulling overall concentrations down. The determinant of these two NOx regimes is the ratio of summed VOCs (weighted by reactivity) to NOx (5).

Our model attempts to account for the potential existence of both high- and low-NOx emissions areas across the study region and represent in a heuristic way some of the above chemistry by including $ln(NOx)$, $ln(NMVOC)$, and the ratio of $ln(NMVOC)$: $ln(NOx)$ (unweighted) in the regression. [Note: VOCs typically include methane, a greenhouse gas that has increased tremendously at global levels over the past decades, but is not usually part of local/regional smog events. It has a fairly uniform global distribution, a longer lifetime than many SLCPs, and is less reactive than many other VOCs. Furthermore, methane is produced during rice cultivation, making it endogenous. We therefore only use NMVOCs (nonmethane VOCs) in this analysis.] At high NOx concentrations, ozone formation is more sensitive to NMVOCs in general (the reaction is NMVOC-limited, and increases in NOx may result in net titration of O_3); at lower NOx concentrations, increases in either NOx or NMVOCs should lead to the formation of ozone (and a decrease in yields). However, the NMVOC:NOx ratio determines the limiting precursor at any given VOC and NOx level. The likelihood of high-NOx regimes in the region is indicated by modeling studies (6, 7), and we find evidence of both NOx regimes in our analysis, as shown in Figs. 2 and 4 and discussed in the main text. (We also conducted the same analysis with different ozone precursor specifications; see below.)

To further inform our model specification, we examined the existing historical data on tropospheric ozone and ozone precursor concentrations in Europe (Fig. 2). Using the European Environment Agency's AirBase database (8), we found the sites and years with valid annual concentration measurements of both ozone and ozone precursors. We then examined the functional relationship between ozone, NOx, total VOCs, and VOC:NOx using this restricted dataset (n = 57 site years). The fit between O_3 and the logarithm of precursor concentrations (for both NOx and VOCs independently, and for the ratio term) was much better than the linear fit. Nevertheless, one can see that, for these sites, an empirical NOx threshold for low- and high-NOx regimes can be determined (~30 μg NO_2/m^3): in the low-NOx regime, O_3 concentrations increase slightly or remain flat with increasing NOx; in the high-NOx regime, O_3 concentrations drop dramatically with increasing NOx (ozone-titrating). We divided the data into low and high NOx to examine the O_3-NOx-VOC relationship in these two regimes. [Note: Most of these sites are urban and are therefore likely in the high NOx regime (i.e., ozone-titrating). This can be seen in the ratio of observations above and below the high-NOx threshold.]

We looked at the equation: $O_3 \sim ln(NOx) + ln(VOC) + [ln(VOC){:}ln(NOx)]$ for high- and low-NOx regimes. At low-NOx concentrations, both NOx and VOCs are statistically significant predictors of ozone concentrations, and the coefficients for $ln(NOx)$ and the $ln(VOC){:}ln(NOx)$ ratio are positive. For high NOx concentrations, only NOx is a statistically significant predictor of ozone concentrations, with a negative coefficient. (For the full sample, the coefficients mimic the high-NOx subsample, but with a lower R^2 value, which makes sense given the urban location of most sites in the sample.)

In our analysis we used estimated emissions in lieu of concentrations, because no long-term records of ozone and ozone precursor concentrations exist for India. This analysis therefore assumes that concentrations are proportional to emissions; future work should probe this relationship directly. We also consider only total NMVOC emissions, without accounting for their relative reactivity.

Alternative Model Specifications. ***Consequences of an emissions-based approach.*** As discussed above, emissions are related—but not equivalent—to concentrations, and it is concentrations of BC and ozone that determine radiation changes and plant toxicity exposure, respectively. Using emissions variables (which are themselves estimates constructed from bottom-up technology surveys) as proxies for concentrations may result in either overestimation (by not accounting for deposition, precipitation, and so forth) or underestimation (because of undercounting in emissions inventories) of impacts. Once a reasonable time series of ozone and precursor concentrations exists, the relationship between SLCP emissions, direct and diffuse radiation fractions, and ozone concentrations can be more fully explored. Future research on crop yield impacts will likely use a two-step process, whereby emissions are related to radiation and ozone, which are then related to yields (e.g., a two-stage least squares estimation, not a dose–response estimate).

Climate and pollution interconnectedness. One of the main difficulties in using panel regression analysis to tease out the impacts of SLCPs on yields is the interconnected nature of emissions and climate variables. As mentioned in the main text, SLCPs have their own independent impacts directly on plant growth (ozone) and via surface radiation changes (aerosols); they also impact regional and global climate, which is then in turn reflected in temperature, precipitation, and radiation changes. Beyond the aerosol indirect and semidirect effects, there are additional interactions among the predictor variables that are not addressed in this study. For example: the rate of formation of tropospheric ozone depends on temperature and radiation, as well as the emission of ozone precursors; the presence of tropospheric ozone also alters surface radiation. For simplicity, and because of lack of degrees of freedom, we do not include these secondary interaction terms.

Carbon monoxide and alternate ozone specifications. We conducted our analysis with several variations on the ozone precursor specifications presented in the main text and this *SI Text*. For example, we substituted carbon monoxide for NMVOCs (and an analogous CO:NOx ratio). We also ran a variation using CO+NMVOC. Our results are robust to such changes; the differences on all are within several percentage points (some larger, some smaller). This finding makes sense, as rising CO levels are linked to changes in background ozone but are not thought to contribute as much to the spatial heterogeneity of surface ozone documented over this region. Future research can leverage the increasing network of surface ozone measurements as well as remote sensing of different species. The alternate ozone specifications presented in Fig. S10 are:

i) *ln(NOx)* only → a simple model using only NOx emissions;
ii) *ln(NMVOC)* only → models with only NMVOC emissions;
iii) *ln(NOx) + ln(NMVOC):ln(NOx)* → only NOx and the ratio of NMVOCs to NOx;
iv) *ln(NMVOC):ln(NOx) + ln(BC):ln(SO_2)* → only the ratios of ozone precursors and the ratio of absorbing to scattering aerosols;
v) *ln(NOx+NMVOC) + ln(NMVOC):ln(NOx) + ln(BC+SO_2) + ln(BC):ln(SO_2)* → grouped aerosols, grouped precursors, and ratios;
vi) The main model presented in the paper, but with year fixed effects as opposed to linear and quadratic time trends. As expected, the addition of year fixed effects swallows much of the interannual variation in climate.

In addition, models using only NMVOCs, models using non-logged versions of variables, models incorporating CO both individually and as part of the VOC:NOx ratio, and models incorporating organic carbon individually and as part of aerosol totals show very similar results.

Alternative climate and emissions data. As a robustness check, we ran our analysis with alternative climate and emissions datasets. First, we used the temperature and precipitation data from the Climatic Research Unit at East Anglia (half-degree data from CRUTS3.21) (9). Based on findings from previous analyses that showed different crop sensitivity to minimum and maximum temperatures, we also ran our model with T_{min} and T_{max} (10). Finally, we used a new aerosols inventory of BC, organic carbon, and sulfur dioxide (from ref. 11) to check inventory sensitivity. The Lu and Streets inventory (Fig. S11) only begins in 1996; we merged these data with Regional Emissions Inventory in Asia (REAS) data by scaling so that values in 1996 were equal. As shown in Fig. S12, our findings are not sensitive to different climate specifications; the use of the Lu et al. (11) data reduce the magnitude of impacts but maintains the same state-by-state pattern. The overall scale of discrepancy between the inventories (e.g., statewide differences in 1996 data) may explain some of this change.

Carbon dioxide (CO_2) fertilization. We do not explicitly include any measures of CO_2 fertilization in our model. Rather, these effects are aliased into the time trends. Inclusion of CO_2 fertilization directly in our model would be problematic because CO_2 is well-mixed in the atmosphere: because this study uses exposure metrics averaged over crop growing area and growing season, exposure trends are similar over the entire growing area, and effects on each crop should likewise be fairly constant. Nevertheless, it is possible to estimate the average CO_2 impact. Free-air CO_2 enrichment experiments on C_3 crops (including rice and wheat) estimate a 14% increase in crop yields when ambient CO_2 is increased from 367 ppm to 583 ppm, or 0.065% yield change per 1-ppm increase in CO_2 (1, 12). Over the course of this study, average CO_2 concentrations increased from 337 ppm to 390 ppm (keelingcurve.ucsd.edu), which would correspond to a yield increase of just under 3.5%. In certain states, this result offsets the direct temperature and precipitation effects, but does not offset the pollution impacts. Moreover, because CO_2 is emitted in the same combustion processes as aerosols (e.g., coal combustion) and ozone precursor compounds (e.g., transportation), our study points to the further complications in isolating CO_2 impacts on crop yields.

Alternative time controls. Several previous statistical panel studies of climate impacts on yields include year fixed effects (FE), which account for events (like economy-wide shocks) affecting the entire study region in given years. We present results of our model with the inclusion of year FE in Fig. S10. The trends are similar, but the overall magnitude of SLCP impacts is larger. When year FE are included, climate impacts are predictably smaller given that the year FE consume much of the variation in the climate signal. As this reduction in signal-to-noise can magnify any measurement or data errors, we choose to omit year FE in our main analysis (13).

Kharif-only analysis. We group our analysis by crop under the assumption (informed by chamber and field studies) that the relationship between SLCPs and crop yields should be crop-specific. (That is, even though we include both rabi rice and kharif rice states in our rice analysis, the climate and pollution variables are averaged over the particular state-crop season.) However, to verify that the inclusion of the two main rabi-producing states is not driving the rice results (e.g., because different cultivars are used in the two seasons or because SLCP impacts are expected to be higher during the dry season), we also present kharif-only analysis in Fig. S13. Results are similar, though of a slightly smaller magnitude.

Model Limitations. ***Model training.*** To illustrate that our results are not being driven by particular years or states, we ran our wheat analysis with a subset of data (even years). We then applied those coefficients to the rest of the data (odd years). The results are shown in Fig. S14.

Explanatory power of different variables. The inclusion of state-specific time trends in our model effectively detrends the data; our model thus asks how much of the variation in year-to-year demeaned yields (e.g., Figs. S2 and S3) is explained by the fluctuations in demeaned climate and emissions variables. The relative importance of the time trends can be seen by first regressing the yield, climate, and pollution variables on the state-specific time trends (i.e., explicitly detrending them) and then regressing the yield residuals on the climate and pollution residuals. The coefficients for the explanatory variables will be identical (Frisch–Waugh–Lovell theorem). By comparing these two regressions, we find that the state-specific time trends explain most (about 89%) of the variation in yields. In addition, we can compare a regression of the yield residuals on climate residuals (alone) versus both climate and pollution residuals to compare whether (and how much) the pollution variables add to the model explanatory power. We found that the explanatory power of the full climate-and-pollution model is better than a model with only climate variables and no pollution variables. Table S2 summarizes these results; the detrended relationship is also shown in the inset of Fig. S14.

These results are not surprising. That is, the pollution variables increase the power of the year-to-year predictions, but not by all that much, in part because year-to-year fluctuations aren't that large in the emissions variables (as seen from the time series plots of emissions in Figs. S5–S7). Put another way, the signal-to-noise ratio for the pollution variables is low. This analysis illustrates the need for larger studies over more widely varying pollution regimes or the leveraging of natural experiments that produce greater year-to-year variation in emissions. In addition, a finer-grained look at management practices may help gain leverage on the remaining variation.

Collinearity. In addition to low signal-to-noise for the emissions variables, our analysis is limited because of multicollinearity, or the strong linear correlation of independent variables in a regression analysis (in this case, the emissions variables, which are all fairly monotonically increasing over time) (Figs. S5–S7, S11, and Table S3). The presence of multicollinearity does not undermine the reliability of the model as a whole (e.g., results in Fig. 3), but it affects our ability to distinguish with certainty the individual impact of the correlated variables, as the variances are inflated. It is for this reason that we are unable to quantify with certainty the relative impacts of aerosols versus ozone within SLCP impacts. In general, the antidote to multicollinearity is more data, adding for example, other countries to a dataset or undertaking analysis at a smaller unit of scale. The latter is only a limited option in this case, as relating local emissions to local yield changes would become invalid at a smaller scale (because of shorter-range pollutant transport). However, expanding the analysis to include other regions of the world (as data become available) points to a promising future avenue of research.

1. Lobell DB, Schlenker W, Costa-Roberts J (2011) Climate trends and global crop production since 1980. *Science* 333(6042):616–620.
2. Auffhammer M, Ramanathan V, Vincent JR (2006) Integrated model shows that atmospheric brown clouds and greenhouse gases have reduced rice harvests in India. *Proc Natl Acad Sci USA* 103(52):19668–19672.
3. Auffhammer M, Ramanathan V, Vincent J (2011) Climate change, the monsoon, and rice yield in India. *Clim Change* 111(2):411–424.
4. Chung CE, Ramanathan V, Decremer D (2012) Observationally constrained estimates of carbonaceous aerosol radiative forcing. *Proc Natl Acad Sci USA* 109(29):11624–11629.
5. Sillman S (1999) The relation between ozone, NOx and hydrocarbons in urban and polluted rural environments. *Atmos Environ* 33(12):1821–1845.
6. Van Dingenen R, et al. (2009) The global impact of ozone on agricultural crop yields under current and future air quality legislation. *Atmos Environ* 43(3):604–618.
7. Avnery S, Mauzerall DL, Liu J, Horowitz LW (2011) Global crop yield reductions due to surface ozone exposure: 2. Year 2030 potential crop production losses and economic damage under two scenarios of O_3 pollution. *Atmos Environ* 45(13):2297–2309.
8. European Environment Agency Topic Centre on Air Pollution and Climate Change Mitigation, AirBase, version 6.0. Available at acm.eionet.europa.eu/databases/airbase. Accessed February 25, 2013.
9. Climatic Research Unit, High-Resolution Gridded Climate Datasets (CRU TS3.21). Available at www.cru.uea.ac.uk/cru/data/hrg. Accessed May 5, 2014.
10. Welch JR, et al. (2010) Rice yields in tropical/subtropical Asia exhibit large but opposing sensitivities to minimum and maximum temperatures. *Proc Natl Acad Sci USA* 107(33):14562–14567.
11. Lu Z, Zhang Q, Streets DG (2011) Sulfur dioxide and primary carbonaceous aerosol emissions in China and India, 1996–2010. *Atmos Chem Phys* 11:9839–9864.
12. Ainsworth EA, Long SP (2005) What have we learned from 15 years of free-air CO_2 enrichment (FACE)? A meta-analytic review of the responses of photosynthesis, canopy properties and plant production to rising CO2. *New Phytol* 165(2):351–371.
13. Fisher AC, Hanemann WM, Roberts M, Schlenker W (2012) The economic impacts of climate change: Evidence from agricultural output and random fluctuations in weather. *Am Econ Rev* 102:3749–3760.

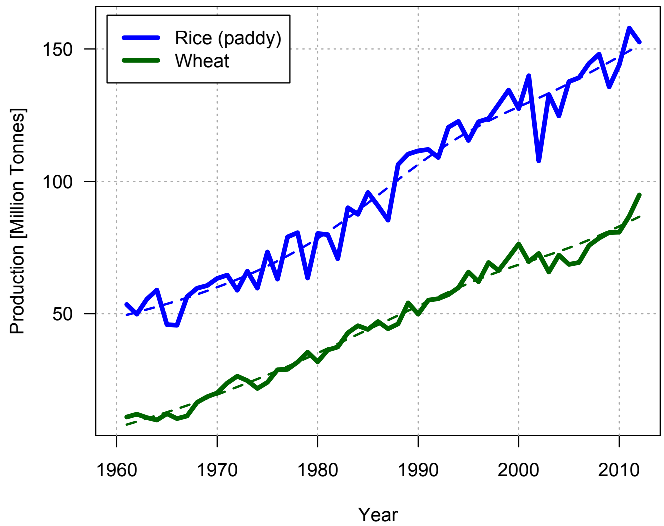

Fig. S1. Historic wheat and rice production in India, 1961–2012.

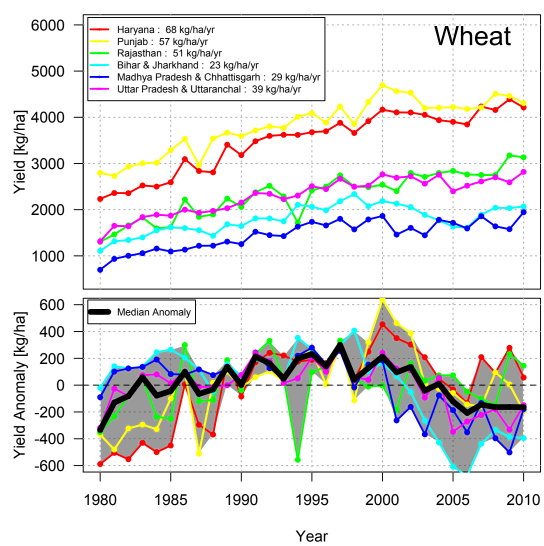

Fig. S2. (*Top*) Wheat yields in the main wheat-producing states in India. (*Bottom*) Detrended wheat yields, showing deviation from fitted state-specific linear trends. Data from IndiaStat.com (1).

1. Datanet India, IndiaStat. Available at www.indiastat.com. Accessed July 17, 2012.

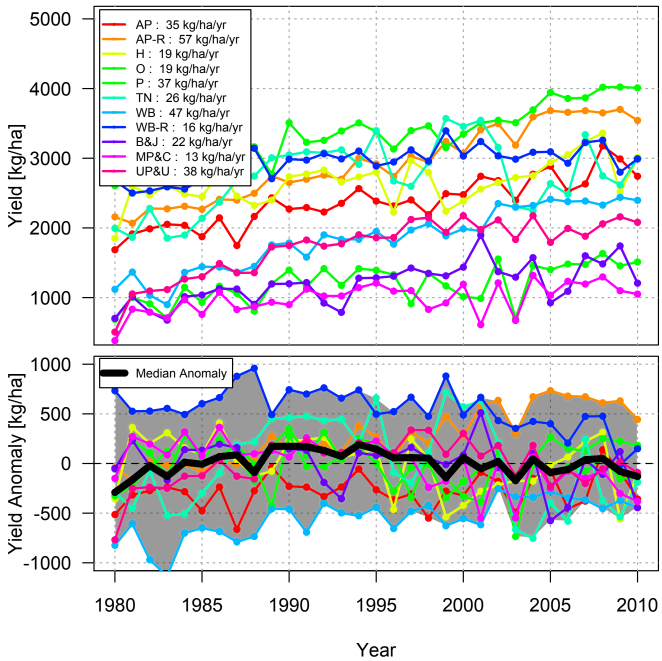

Fig. S3. (*Top*) Rice yields in the main rice-producing states in India. (*Bottom*) Detrended rice yields, showing deviation from fitted state-specific linear trends. Data from IndiaStat.com (1).

1. Datanet India, IndiaStat. Available at www.indiastat.com. Accessed July 17, 2012.

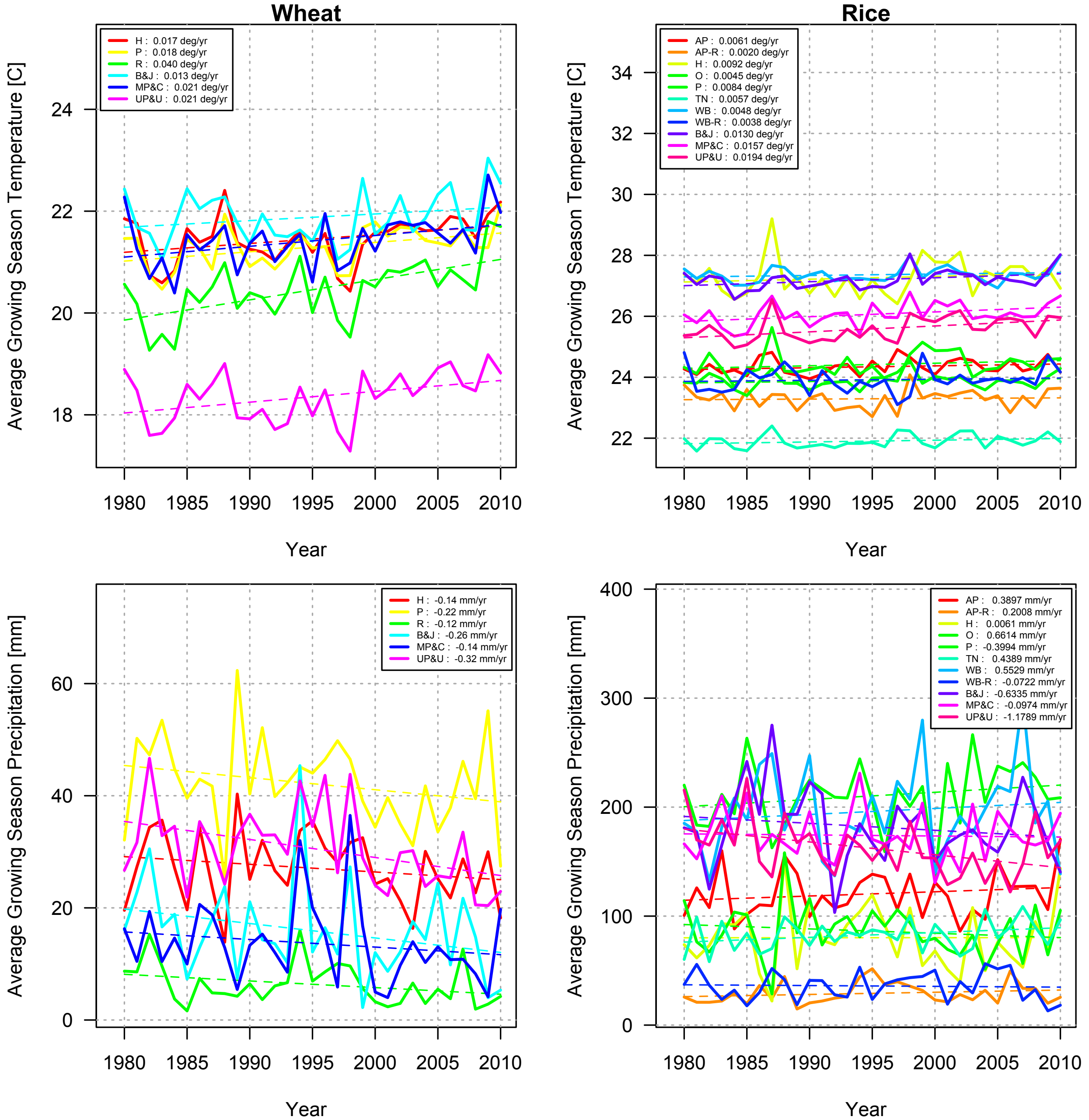

Fig. S4. Growing season temperature and precipitation trends for major rice- and wheat-producing states in India, 1980–2010.

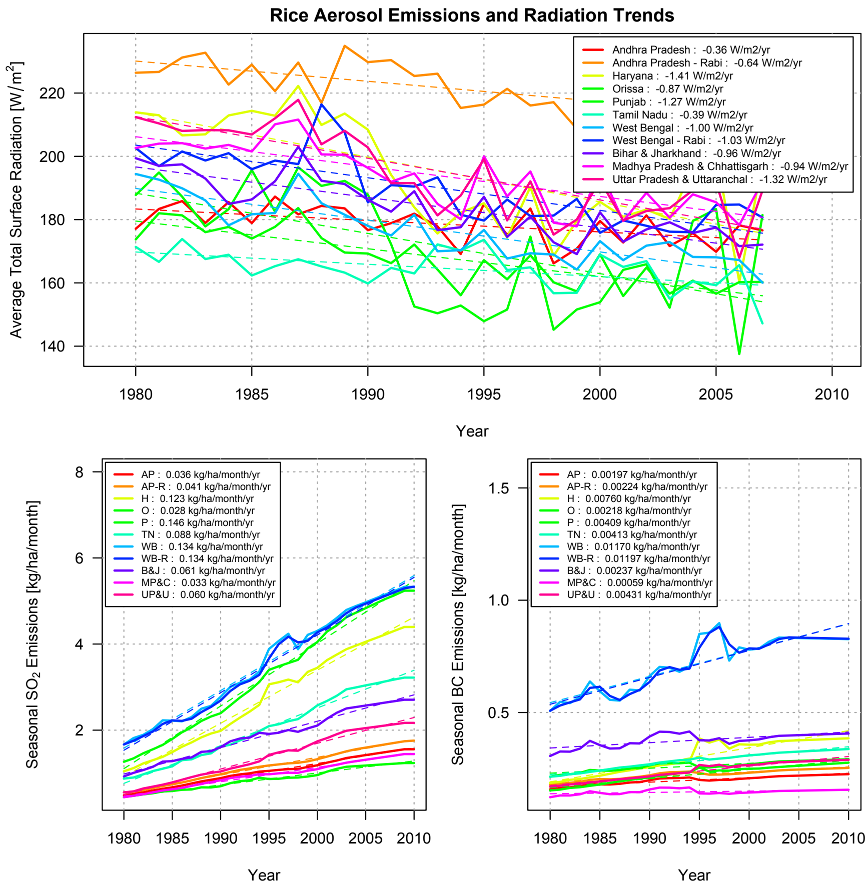

Fig. S5. (*Top*) Trends in total average daily surface radiation over the kharif rice growing season, by state. State-specific linear dimming trends (fitted slopes) shown in the legend. Data from the World Radiation Data Centre (1). (*Bottom*) Emissions of (*Left*) SO_2 and (*Right*) BC by state over the season, with state-specific linear emissions trends (fitted slopes) shown in the legend. Data from the REAS emissions inventory (2).

1. World Radiation Data Center (WRDC), Global Radiation Data. Available at wrdc.mgo.rssi.ru. Accessed June 9, 2011.
2. Ohara T, et al. (2007) An Asian emission inventory of anthropogenic emission sources for the period 1980–2020. *Atmos Chem Phys* 7:4419–4444.

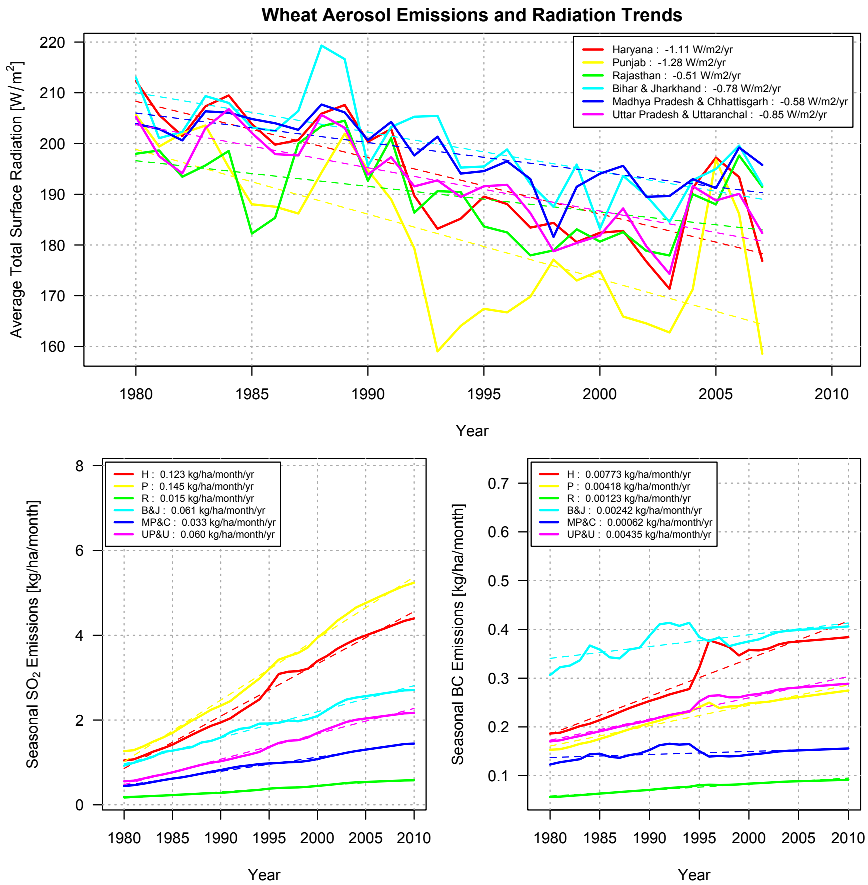

Fig. S6. (*Top*) Trends in total average daily surface radiation over the wheat growing season, by state. State-specific linear dimming trends (fitted slopes) shown in the legend. Data from the World Radiation Data Centre (1). (*Bottom*) Emissions of (*Left*) SO_2 and (*Right*) BC by state over the season, with state-specific linear emissions trends (fitted slopes) shown in the legend. Data from the REAS emissions inventory (2).

1. World Radiation Data Center (WRDC), Global Radiation Data. Available at wrdc.mgo.rssi.ru. Accessed June 9, 2011.
2. Ohara T, et al. (2007) An Asian emission inventory of anthropogenic emission sources for the period 1980–2020. *Atmos Chem Phys* 7:4419–4444.

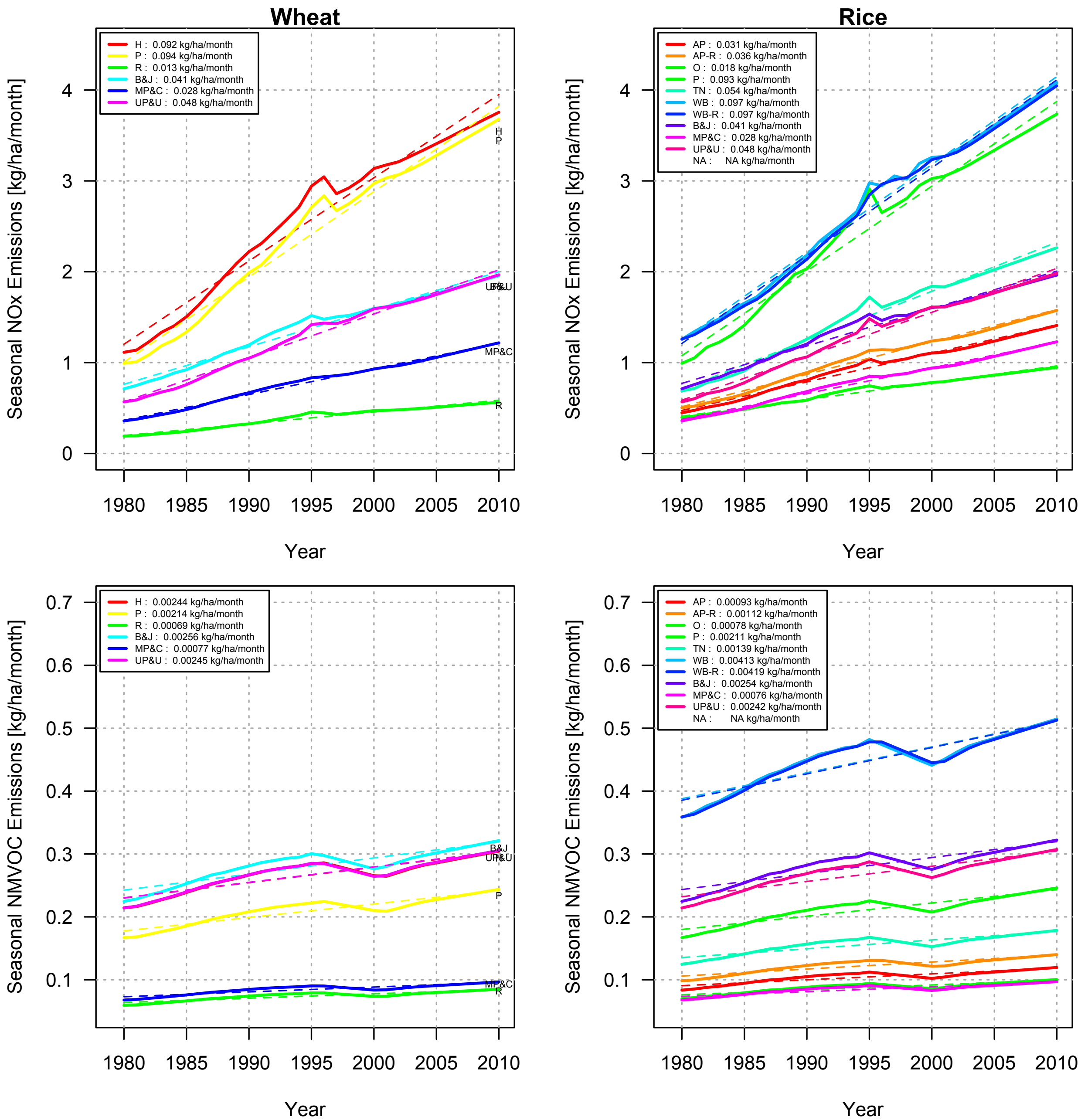

Fig. S7. Trends in NOx and NMVOC emissions for major wheat- and rice-producing states in India, 1980–2010. Data from REAS emissions inventory (1).

1. Ohara T, et al. (2007) An Asian emission inventory of anthropogenic emission sources for the period 1980–2020. *Atmos Chem Phys* 7:4419–4444.

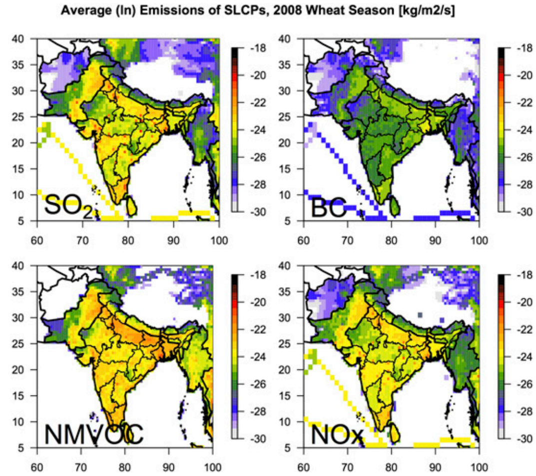

Fig. S8. Average wheat growing season emissions of SO_2, BC, NMVOC, and NOx in 2008. Data from the REAS emissions inventory (1).

1. Ohara T, et al. (2007) An Asian emission inventory of anthropogenic emission sources for the period 1980–2020. *Atmos Chem Phys* 7:4419–4444.

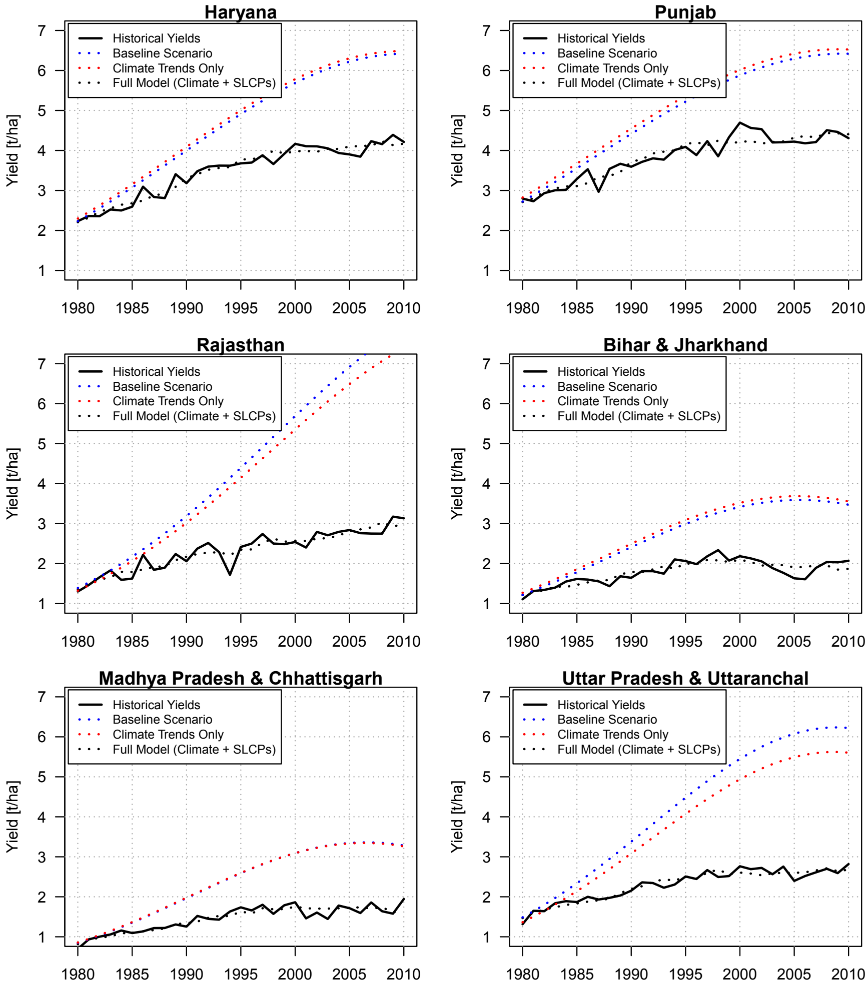

Fig. S9. State-by-state breakdown of impacts of technology/time trends, climate, and pollution for wheat-producing states.

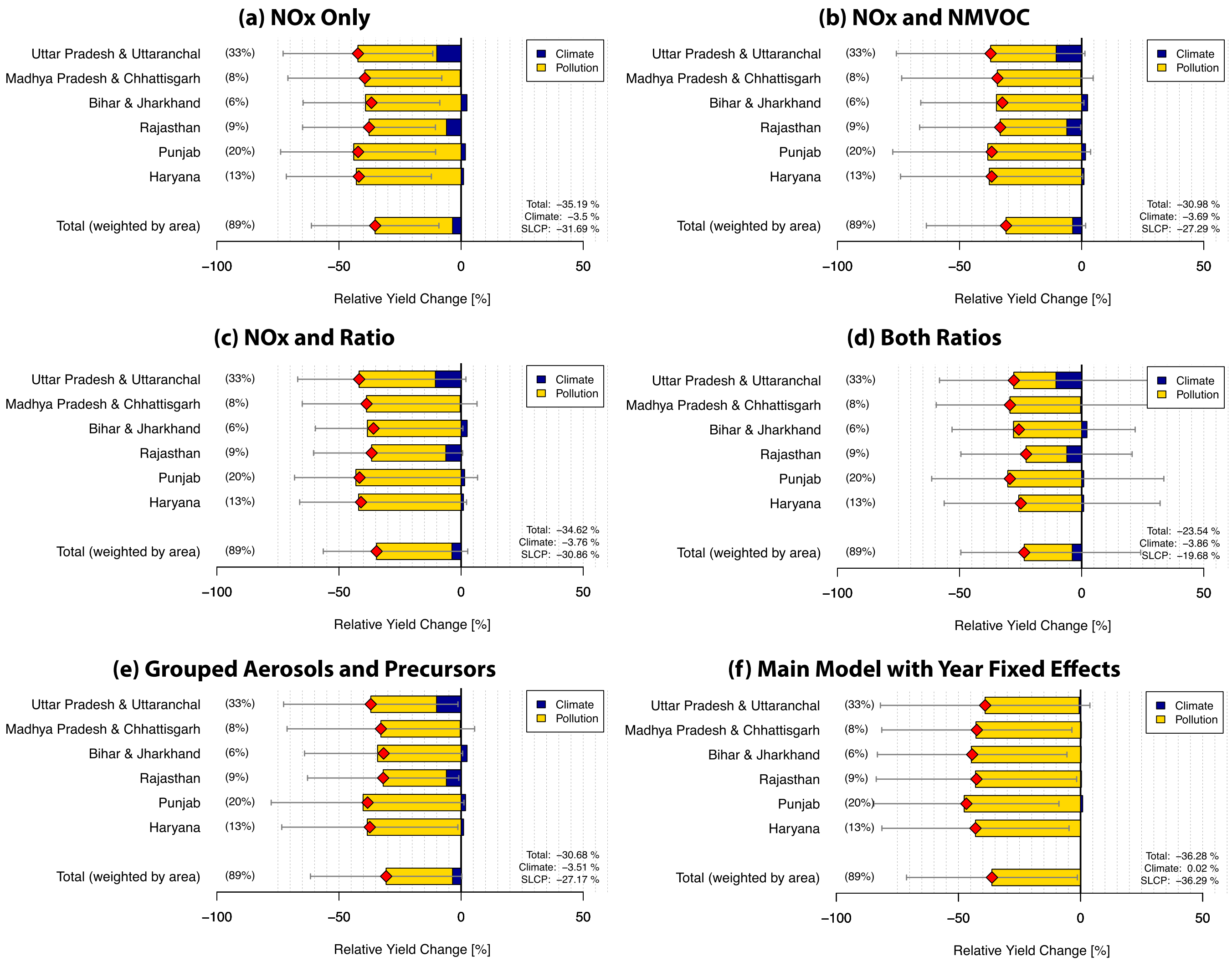

Fig. S10. Alternative model specifications for wheat. These models use different specifications for ozone precursor and aerosol emissions, as shown in the figure legend. Models are described in more detail in *SI Text*.

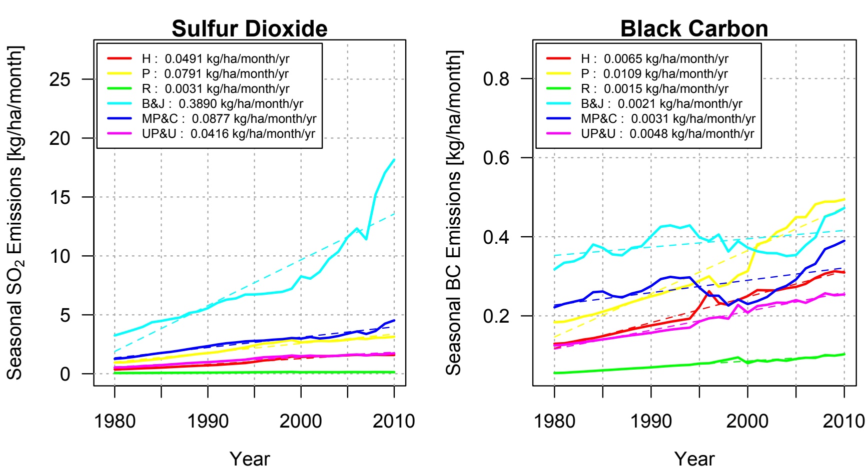

Fig. S11. Emissions trends from Lu and Streets aerosols inventory (1). The inventory begins in 1996; we merged these data with REAS data by scaling so that values in 1996 were equal.

1. Lu Z, Zhang Q, Streets DG (2011) Sulfur dioxide and primary carbonaceous aerosol emissions in China and India, 1996–2010. *Atmos Chem Phys* 11:9839–9864.

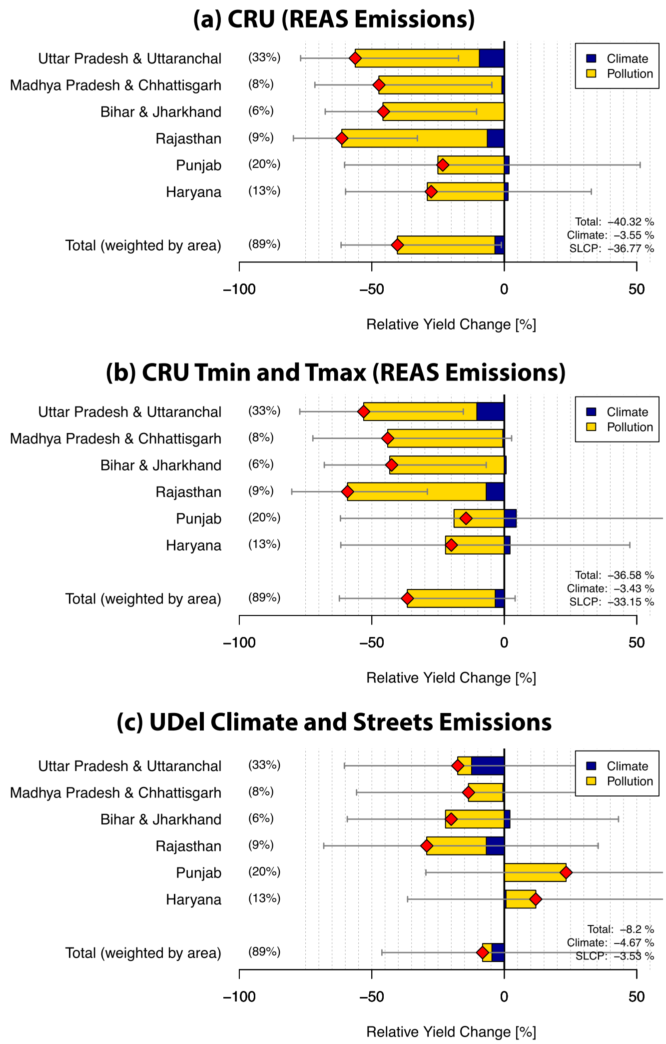

Fig. S12. Analysis with alternative climate and emissions datasets. CRU data are from the Climatic Research Unit at East Anglia; we used half-degree data from CRUTS3.21 (1). The first specification (*A*) replicates the main model presented in the paper, but with CRU data replacing University of Delaware data. The second specification (*B*) uses T_{min} and T_{max}, as recent research has shown that crops are sensitive in different ways to these two quantities (2). The third specification (*C*) uses a different, higher-resolution ($0.1° \times 0.1°$) emissions inventory for the aerosols portion of the model. The Streets inventory of black carbon, organic carbon, and sulfur dioxide (3) begins in 1996; we merged these data with REAS data by scaling so that values in 1996 were equal.

1. Climatic Research Unit, High-Resolution Gridded Climate Datasets (CRU TS3.21). Available at www.cru.uea.ac.uk/cru/data/hrg. Accessed May 5, 2014.
2. Welch JR, et al. (2010) Rice yields in tropical/subtropical Asia exhibit large but opposing sensitivities to minimum and maximum temperatures. *Proc Natl Acad Sci USA* 107(33):14562–14567.
3. Lu Z, Zhang Q, Streets DG (2011) Sulfur dioxide and primary carbonaceous aerosol emissions in China and India, 1996–2010. *Atmos Chem Phys* 11:9839–9864.

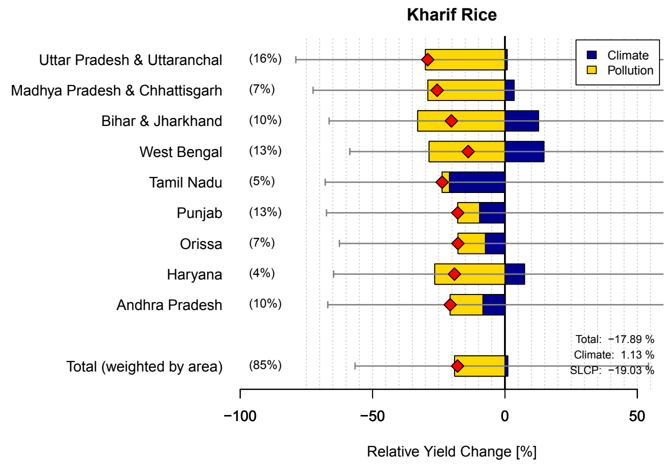

Fig. S13. Main model with only kharif (rainy season) rice.

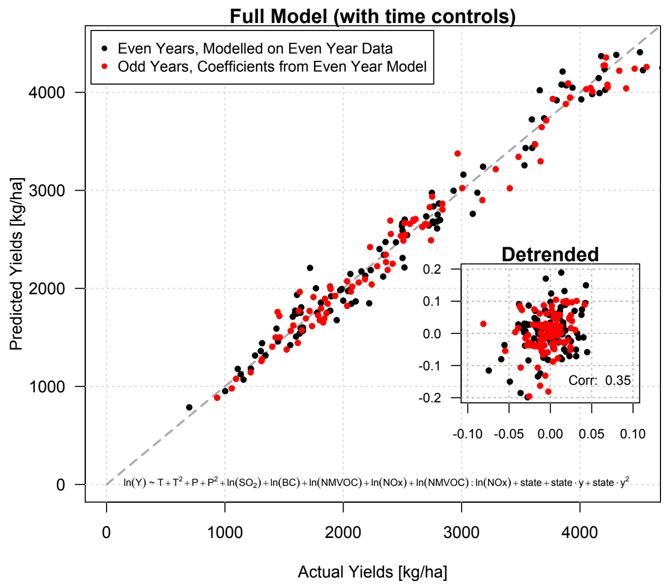

Fig. S14. Even-odd analysis. Main plot shows predicted versus actual wheat yields for model fit to even-year data (black), and predictions (from even-year fit) to odd-year data. *Inset* shows fits from residuals of detrended variables.

Table S1. Regression coefficients for wheat and rice (Eq. 1)

	Wheat	Rice
Variables	ln(Yield)	ln(Yield)
T	−0.051** (0.021)	−0.552 (0.601)
T^2	−0.000 (0.005)	−0.130 (0.492)
P	−0.015 (0.015)	−0.040 (0.026)
P^2	0.002 (0.006)	0.007 (0.017)
ln(BC)	0.247 (0.182)	0.193 (0.332)
$ln(SO_2)$	−0.756*** (0.238)	−0.562 (0.532)
ln(NOx)	−7.228** (3.511)	0.483 (7.875)
ln(NMVOC)	7.111** (3.294)	0.328 (7.403)
ln(NOx): ln(NMVOC)	162.145** (76.157)	−5.462 (170.982)
Year	0.035*** (0.009)	0.021 (0.016)
$Year^2$	−0.002*** (0.000)	−0.000 (0.001)
Constant	−168.392** (81.200)	25.634 (185.259)
Observations	186	341
R^2	0.9999	0.9998
rmse	0.0704	0.128

SEs in parentheses; ***$P < 0.01$, **$P < 0.05$, *$P < 0.1$. State-specific intercepts and linear and quadratic time coefficients not shown for brevity. Coefficients for T and T^2, P and P^2, and ozone precursors must be interpreted collectively. For wheat, temperature is statistically significant at 90% (P = 0.051), aerosols are significant at 99% (P = 0.003), and ozone precursors are significant at 90% (P = 0.056). For rice, temperature is statistically significant at 95% (P = 0.016), aerosols are not statistically significant, and ozone precursors are significant at 99% (P = 0.005).

Table S2. Explanatory power of time trend, climate, and pollution variables

Model	Adjusted R^2	rmse
Full model	0.9687	0.0704
Detrended model (climate and pollution variables)	0.0746	0.0669
Detrended climate-only model	0.0346	0.0683

Table S3. Correlations between state-level variables for wheat analysis

	Year	Temperature	Precipitation	$ln(SO_2)$	*ln(BC)*	*ln(NOx)*	*ln(NMVOC)*
Year	1.0000						
Temperature	0.1110	1.0000					
Precipitation	−0.0970	−0.1952	1.0000				
$ln(SO_2)$	0.4667	0.2996	0.5766	1.0000			
ln(BC)	0.2485	0.2066	0.4268	0.8532	1.0000		
ln(NOx)	0.4560	0.2285	0.6026	0.9848	0.8256	1.0000	
ln(NMVOC)	0.1407	−0.0536	0.5734	0.7781	0.9054	0.7990	1.0000